

Evaluation of Dynamic spin structure factor for the spin-1/2 XXZ chain in a magnetic field

Jun Sato, Masahiro Shiroishi and Minoru Takahashi

Institute for Solid State Physics, University of Tokyo, Kashiwa, Chiba 277-8581, Japan

(Received November 19, 2018)

Transition rates and dynamic spin structure factor at zero temperature for the spin-1/2 XXZ chain at critical regime in a magnetic field are numerically evaluated in terms of the exact determinant representations for the form factors and norms of the Bethe eigenstates. We have seen that the transition rates converges toward the constant function with the value 1 in the limit $\Delta \rightarrow 0$. The observed critical exponent of the singularity at the lower boundary is compared with the one predicted from the conformal field theory. We confirm that they are in good agreement. Further we have discovered that a small peak emerges near the upper boundary in the line shape of $S(q, \omega)$ for $0 < \Delta < 1$.

KEYWORDS: Bethe ansatz, XXZ model, dynamic spin structure factor, CFT

1. Introduction

Since Bethe¹ in 1931 formulated the method (Bethe ansatz) for obtaining the exact eigenvalues and eigenvectors of the one-dimensional spin-1/2 Heisenberg model, it has been extensively generalized to study the excitations and the thermodynamics of the model exactly.² However, from the point of view of the dynamics of Heisenberg antiferromagnetic chains, only approximate results had been obtained until recently, partly due to the lack of the exact expression for the form factors.

Heisenberg antiferromagnetic chains are realized in quasi-one-dimensional magnetic insulators, such as, $\text{Cu}(\text{C}_4\text{H}_4\text{N}_2)(\text{NO}_3)_2$,³ and KCuF_3 .⁴ Dynamic spin structure factor $S(q, \omega)$, which is the Fourier transform of dynamical correlation functions, is of considerable importance, since they are directly comparable with inelastic neutron scattering experiments of these quasi one-dimensional substances.⁶

In 1967 Niemeijer obtained an exact expression of $S(q, \omega)$ for the spin-1/2 XY model at any temperature.⁵ It is the special case ($\Delta = 0$) of XXZ model, where all the correlation functions can be calculated by Jordan-Wigner transformation. Unfortunately this exact calculation can not be extended for general case of $\Delta \neq 0$, and only approximate evaluations of $S(q, \omega)$ had been attempted.⁷ It was worth noting, therefore, that an analytical result for the two-spinon dynamic spin structure factor for the spin-1/2 massive XXZ model ($\Delta \geq 1$) in zero magnetic field was obtained⁸⁻¹⁰ from the multiple integral representation for form factors,¹¹ which is based on the infinite dimensional symmetries of the quantum affine algebra $U_q(\hat{sl}(2, \mathbf{C}))$.

However, this analytical calculation is not applicable to the case with nonzero magnetic field. Karbach et al. classified the dynamically dominant excitations of the spin-1/2 XXX Heisenberg model ($\Delta = 1$) in a magnetic field. They subsequently calculated their transition rates pertaining to dynamic spin structure factor, directly from the Bethe wave functions for finite chains with up to $N = 32$ sites.^{12,13} Although solving the Bethe ansatz equations in its own is possible for $N \approx 10^3$, constructing the Bethe wave functions is limited to $N \approx 32$. The problem of this direct calculation lies in the evaluation of the sum over the $r!$ magnon permutations in the coefficients of the coordinate Bethe wave functions, where r is the number of the down spins.

Quite recently, this problem was solved by the novel work of Kitanine et al., who derived the exact determinant representation for the form factors of local spin operators for arbitrary finite systems.¹⁴ In the framework of the algebraic Bethe ansatz,¹⁵ they have found that any local operators can be written as the elements of the quantum monodromy matrix. Consequently the calculation of form factors reduces to that of scalar products between a Bethe state and an arbitrary state, which has a determinant representation. Then it enables us to calculate transition rates directly from the solution of Bethe ansatz equations, without constructing the Bethe wave functions.

Biegel et al. calculated dynamic spin structure factors for chains with the order $N \approx 10^3$ using this determinant representation in the case of XXX Heisenberg chain in a magnetic field¹⁶ and in the case of XXZ Heisenberg chain at critical regime in zero magnetic field.^{17,18} As much as these calculations are still for the finite systems, we can deal with much larger system sizes than in the past.

In this paper, as an extension of these works, we shall generalize the work by Biegel et al. and evaluate dynamic spin structure factors for the spin-1/2 XXZ chain in a magnetic field. Under the existence of a magnetic field, only the XXX case has been dealt with so far.

2. Bethe ansatz

Let us consider the one-dimensional spin-1/2 XXZ model with periodic boundary conditions in a magnetic field

$$H = J \sum_{n=1}^N \left\{ S_n^x S_{n+1}^x + S_n^y S_{n+1}^y + \Delta (S_n^z S_{n+1}^z - \frac{1}{4}) \right\} - h \sum_{n=1}^N S_n^z, \quad (1)$$

where $J > 0$ is the coupling constant, $S^{x,y,z} = \frac{1}{2} \sigma^{x,y,z}$, Δ is the anisotropy parameter and h is the external magnetic field applied to the positive direction of z -axis. $\sigma^{x,y,z}$ represents the standard Pauli matrices.

It is exactly solved by Bethe ansatz method. Bethe eigenstates with r down spins are constructed by a set of rapidities $\{z_1, \dots, z_r\}$, which is a solution of Bethe ansatz equations

$$N \tan^{-1}[\cot \frac{\gamma}{2} \tanh z_i] = \pi I_i + \sum_{j \neq i}^r \tan^{-1}[\cot \gamma \tanh(z_i - z_j)],$$

$$i = 1, \dots, r, \quad (2)$$

where the parameter γ is related to the anisotropy Δ as $\gamma = \cos^{-1} \Delta$. I_i are Bethe quantum numbers, which have integer values for odd r and half odd integer values for even r . The total momentum and energy eigenvalues are given by

$$k = \pi r - \frac{2\pi}{N} \sum_{i=1}^r I_i, \quad (3a)$$

$$E = J \sum_{i=1}^r \frac{-\sin^2 \gamma}{\cosh 2z_i - \cos \gamma} - h \left(\frac{N}{2} - r \right). \quad (3b)$$

Every solution of Bethe ansatz equations is uniquely determined by Bethe quantum numbers $I_1 < \dots < I_r$, which provide us the classification of the excitations. The ground state $|G\rangle$ at magnetization $0 \leq M_z \leq N/2$ is specified by the set of $r = N/2 - M_z$ Bethe quantum numbers $I_i = -N/4 + M_z/2 + i - 1/2$.

3. Dynamically dominant excitations

In neutron scattering experiment at sufficiently low temperature, the cross section is considered to be proportional to the dynamic spin structure factor $S(q, \omega)$ at zero temperature, which is defined by the space-time Fourier transform of the dynamical correlation function:

$$\begin{aligned} S_{\mu\bar{\mu}}(q, \omega) &= \frac{1}{N} \sum_{n, n'} e^{iq(n-n')} \int_{-\infty}^{\infty} dt e^{i\omega t} \langle S_n^\mu(t) S_{n'}^{\bar{\mu}}(0) \rangle \\ &= \int_{-\infty}^{\infty} dt e^{i\omega t} \langle S_q^\mu(t) S_q^{\mu\dagger}(0) \rangle \\ &= 2\pi \sum_{\lambda} |\langle G | S_q^\mu | \lambda \rangle|^2 \delta(\omega - \omega_\lambda), \end{aligned} \quad (4)$$

where $(\mu, \bar{\mu}) = (z, z), (+, -), (-, +)$, $\omega_\lambda = E_\lambda - E_G$. E_G and E_λ are the energy eigenvalues of the ground state $|G\rangle$ and one of the excited states $|\lambda\rangle$, respectively. The spin fluctuation operator S_q^μ is defined by

$$S_q^\mu = \frac{1}{\sqrt{N}} \sum_{n=1}^N e^{iqn} S_n^\mu, \quad \mu = z, +, -, \quad (5)$$

for wave numbers $q = 2\pi l/N$, $l = 1, \dots, N$.

In the following, we will focus on the case for the parallel spin fluctuations $(\mu, \bar{\mu}) = (z, z)$, $q = \pi/2$, and for half the saturation magnetic field $M_z = N/4$, $r = N/2 - M_z = N/4$. In the case of XXX model ($\Delta = 1$), it was established that the spectral weight of $S_{zz}(q, \omega)$ is dominated by the set of collective excitations, called "psinon(Ψ)-antipsinon(Ψ^*)" excitations, which is denoted by $\Psi\Psi^*$.¹² Their Bethe quantum numbers are shown in figure 3. The I_i are given by the position of small black circles in each row. The positions of large circles represent the I_i vacancies. The first row represents the ground state $|G\rangle$, whose Bethe quantum numbers are uniformly cofigured at the center.

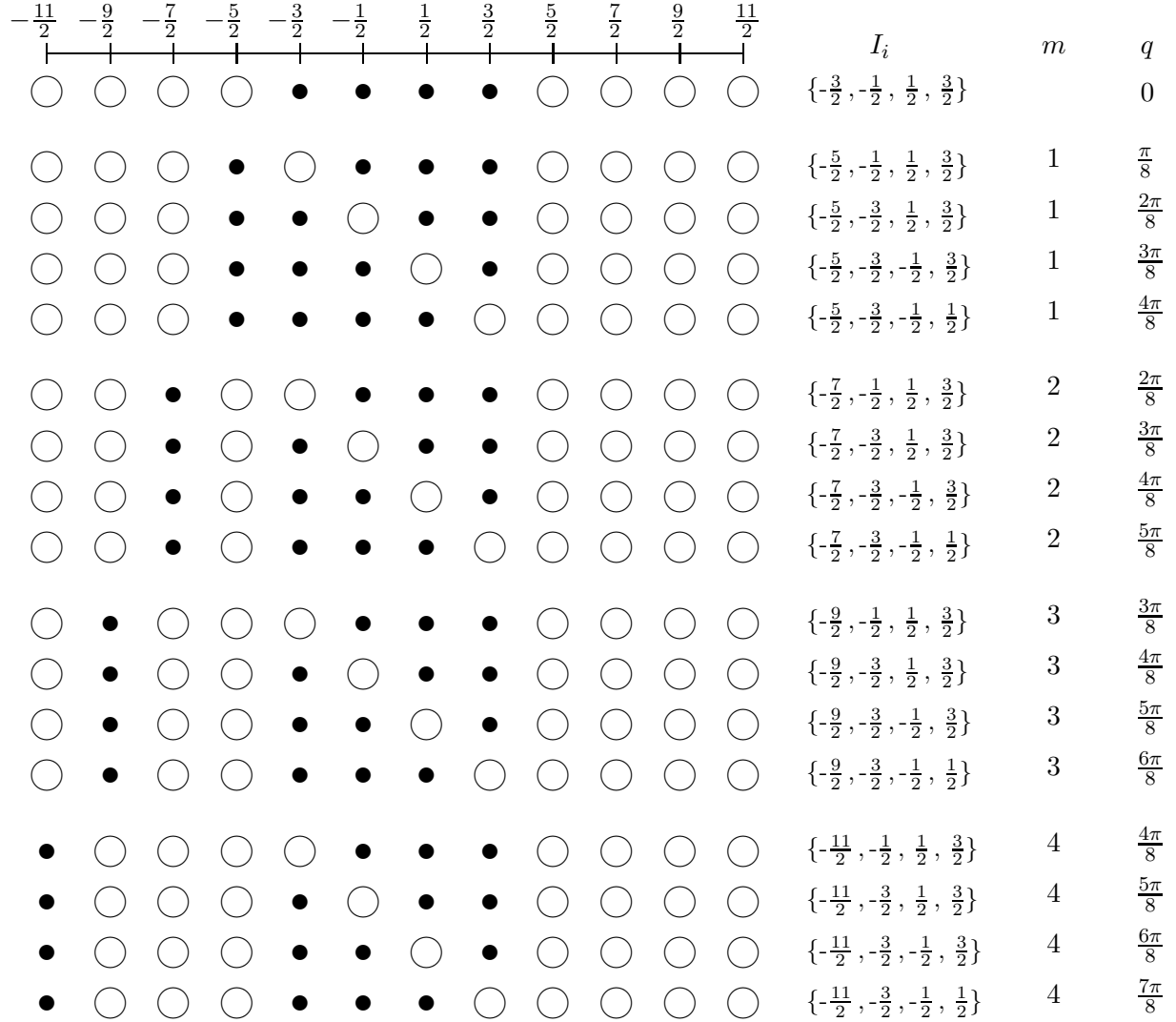


Fig. 1. Configurations of Bethe quantum numbers of psinon-antipsinon excitations for $N = 16$, $M_z = 4$, $r = 4$. I_i are represented by the positions of small black circles. Large circles represent I_i vacancies. The first row represents the ground state $|G\rangle$.

When one of the Bethe quantum numbers of the ground state is moved to the sea of I_i vacancies, it becomes antipsinon. Then it makes a hole in the I_i configurations, which represents the psinon. In this way, we have a set of excitations with two parameters, which is called psinon-antipsinon excitations. We label the $\Psi\Psi^*$ states with the integer parameter m . The state $|m\rangle$ has the Bethe quantum number $I_1 = -r/2 - m + 1/2$.

The relative contribution of psinon-antipsinon excitations is determined by the ratio of the integrated intensity

$$S_{zz}(q) = \int_{-\infty}^{\infty} \frac{d\omega}{2\pi} S_{zz}(q, \omega) = \sum_{\lambda} |\langle G | S_q^z | \lambda \rangle|^2 = \langle G | S_q^z S_{-q}^z | G \rangle \quad (6)$$

Table I. Relative contributions of psinon-antipsinon excitations for $N = 24$, $M_z = r = 6$, $q = \pi/2$.

Δ	$S_{zz}^{\Psi\Psi^*}(\pi/2)$	$S_{zz}(\pi/2)$	Relative contribution(%)
-0.4	0.228545	0.232882	98.1378
-0.3	0.234930	0.237182	99.0504
-0.1	0.245605	0.245782	99.9282
-0.01	0.249581	0.249582	99.9994
0.01	0.250415	0.250417	99.9994
0.1	0.253984	0.254114	99.9489
0.3	0.260983	0.261918	99.6431
0.4	0.264076	0.265574	99.4360
0.5	0.266954	0.269056	99.2189
0.7	0.272230	0.275491	98.8161
0.9	0.277048	0.281247	98.5068
1	0.279318	0.283887	98.3907
1.1	0.281503	0.286378	98.2977
1.5	0.289411	0.295027	98.0965
2.0	0.297553	0.303452	98.0559

and $\Psi\Psi^*$ contribution

$$S_{zz}^{\Psi\Psi^*}(q) = \sum_{\Psi\Psi^*} |\langle G|S_q^z|\Psi\Psi^*\rangle|^2 = \sum_m |\langle G|S_q^z|m\rangle|^2. \quad (7)$$

Relative contributions for various values of Δ are shown in table I. We see they are more than 98% for general Δ . Although the relative contribution actually decreases as the system size N increases, it was shown in Ref.[11] that the relative contribution for the XXX model ($\Delta = 1$) is more than 93% from an extrapolation of the data for $N = 12, 16, 20, 24, 28, 32$. Also we find that the relative contribution is monotonously increasing when we bring down the value of Δ from 1 to 0. Hence we can conclude that the $\Psi\Psi^*$ excitation is dynamically dominant in the whole region $0 < \Delta < 1$.

4. Transition rates and Dynamic spin structure factor

We numerically evaluate the dynamic spin structure factor from the contribution of $\Psi\Psi^*$ excitations:

$$S_{zz}^{\Psi\Psi^*}(q, \omega) = 2\pi \sum_m |\langle G|S_q^z|m\rangle|^2 \delta(\omega - \omega_m). \quad (8)$$

In the thermodynamic limit $N \rightarrow \infty$, it can be represented by the product of the transition rates $M_{zz}(q, \omega_m) = N|\langle G|S_q^z|m\rangle|^2$ and the density of states $D_{zz}(q, \omega_m) = \frac{2\pi}{N} \frac{1}{\omega_{m+1} - \omega_m}$.¹³

From the determinant representations for the form factors and norms of Bethe eigenstates,¹⁴ we have the following formula for transition rates:

$$M_{zz}(q, \omega) = \frac{N^2}{4} \frac{\prod_{j=1}^r \left| \sinh(z_j^0 - \frac{i\gamma}{2}) \right|^2}{\prod_{j=1}^r \left| \sinh(z_j - \frac{i\gamma}{2}) \right|^2} \left| \prod_{j<k}^r \frac{1}{\sinh^2(z_j^0 - z_k^0) + \sin^2 \gamma} \right| \left| \prod_{\alpha<\beta}^r \frac{1}{\sinh^2(z_\alpha - z_\beta) + \sin^2 \gamma} \right|$$

$$\times \frac{|\det(H - 2P)|^2}{|\det \Phi(\{z_j^0\})| |\det \Phi(\{z_j\})|}, \quad (9)$$

where the matrix elements of H , P and Φ are given by

$$\left\{ \begin{array}{l} \Phi(\{z_j\})_{ab} = \begin{cases} \frac{\sin 2\gamma}{\sinh^2(z_a - z_b) + \sin^2 \gamma} & (a \neq b) \\ N \frac{\sin \gamma}{\sinh^2 z_a + \sin^2 \frac{\gamma}{2}} - \sum_{\substack{k=1 \\ k \neq a}}^r \frac{\sin 2\gamma}{\sinh^2(z_a - z_k) + \sin^2 \gamma} & (a = b) \end{cases} \\ H(\{z_j^0\}, \{z_k\})_{ab} = \frac{1}{\sinh(z_a^0 - z_b)} \left(\prod_{j \neq a}^r \sinh(z_j^0 - z_b - i\gamma) - \left[\frac{\sinh(z_b - \frac{i\gamma}{2})}{\sinh(z_b + \frac{i\gamma}{2})} \right]^N \prod_{j \neq a}^r \sinh(z_j^0 - z_b + i\gamma) \right) \\ P(\{z_j^0\}, \{z_k\})_{ab} = \frac{1}{\sinh^2 z_a^0 + \sin^2 \frac{\gamma}{2}} \prod_{k=1}^r \sinh(z_k - z_b - i\gamma). \end{array} \right. \quad (10)$$

$\{z_1^0, \dots, z_r^0\}$ and $\{z_1, \dots, z_r\}$ are the rapidities corresponding to the ground state $|G\rangle$ and one of the $\Psi\Psi^*$ states $|m\rangle$, respectively. To obtain the desired transition rates, we first solve the Bethe ansatz equations (2) for given Bethe quantum numbers I_i , and then substitute the solution to the formula (9).

We rewrite the Bethe quantum numbers I_i of the $\Psi\Psi^*$ state $|m\rangle$ at $q = \pi/2$:

$$\begin{aligned} I_1 &= -r/2 - m + 1/2 \\ I_i &= -r/2 + i - 3/2 \quad (2 \leq i \leq r - m + 1) \\ I_i &= -r/2 + i - 1/2 \quad (r - m + 2 \leq i \leq r) \end{aligned} \quad (11)$$

for $1 \leq m \leq r$

When m increases and approaches toward r , the first Bethe quantum number I_1 gets away from the other I_i configurations, and the transition rate monotonously decreases. At the same time it is getting more difficult to find the solution of the first rapidity z_1 .

In figure 2(b), we plot transition rates $M_{zz}(\pi/2, \omega)$ for $N = 4096$. Also shown in the inset (a) are the excitation spectrum of $\Psi\Psi^*$ states for each Δ . Note that in the XXX case ($\Delta = 1$), the transition rates $M_{zz}(\pi/2, \omega)$ can be observed as a smooth function of ω , which has a singularity at the lower boundary, and converges toward zero at the upper boundary.¹⁶

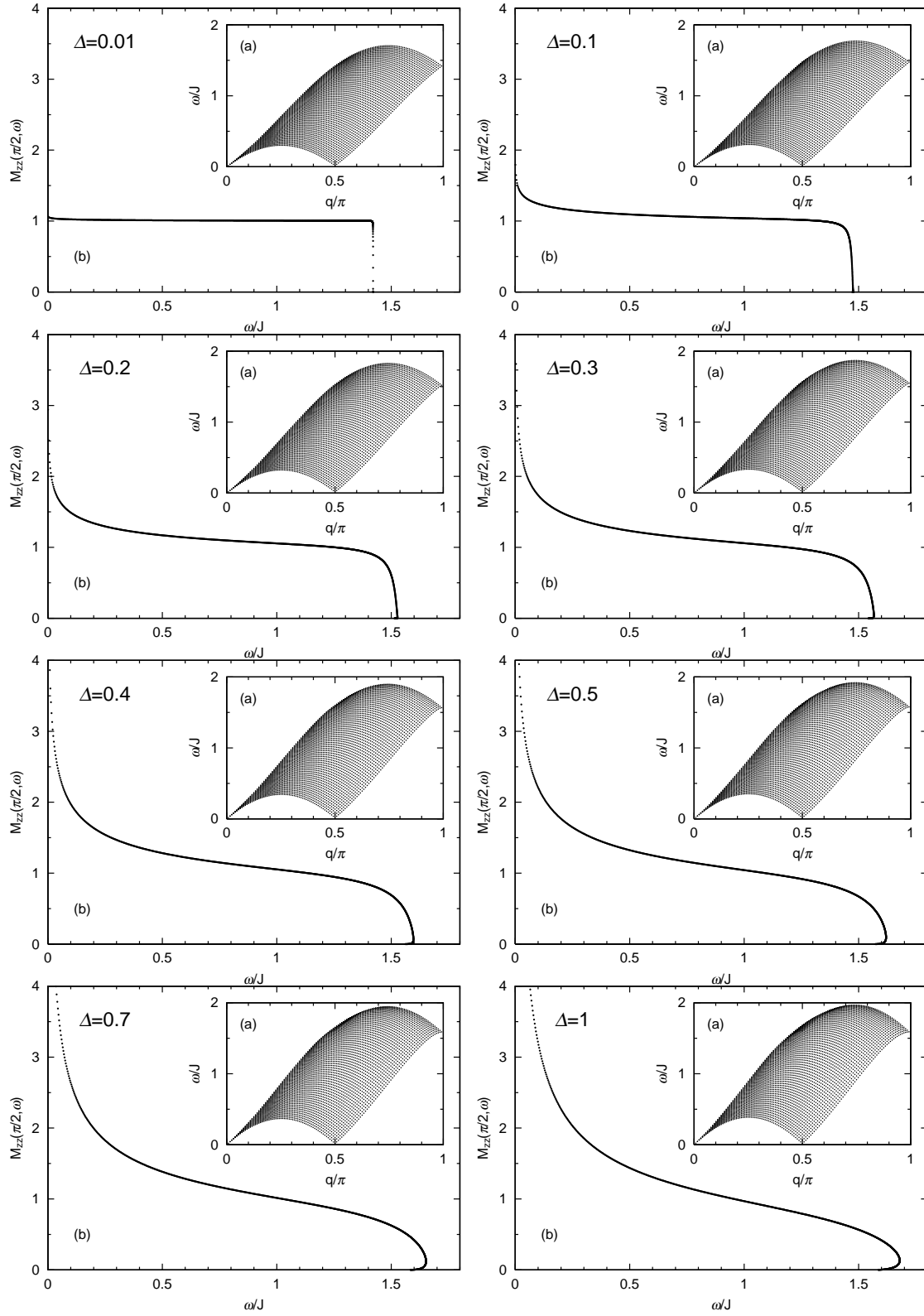


Fig. 2. (a) Energy versus momentum of the psinon-antipsinon excitations at $M_z = N/4$ for $N=256$. (b) Transition rates between the ground state and the psinon-antipsinon excitations at $q = \pi/2$, $M_z = N/4$ for $N=4096$.

Table II. Critical Exponent of the singularity at the lower boundary

Δ	1	0.9	0.7	0.5
Ω_z	4.38286228	4.39050106	4.40585570	4.42060672
$2\pi v$	5.72474288	5.64334684	5.45713287	5.23326627
$2\theta_z$	1.53119969	1.55599192	1.61471447	1.68942549
η_z	1.5313	1.5565	1.6163	1.6923

Δ	0.4	0.3	0.2	0.1	0.01
Ω_z	4.42734708	4.43333735	4.43823777	4.44160837	4.44286904
$2\pi v$	5.10437806	4.96243131	4.80595322	4.63334574	4.46278471
$2\theta_z$	1.73472538	1.78676018	1.84697501	1.91723589	1.99107478
η_z	1.7384	1.7910	1.8516	1.9213	1.9918

In the XXZ case at the critical regime $0 < \Delta < 1$, it can be observed that when we bring close to $\Delta = 0$ starting from $\Delta = 1$, the singularity at the lower boundary has been weakened and at last the function $M_{zz}(\pi/2, \omega)$ converges to the constant function with the value 1.

The critical exponent of the singularity at the lower boundary can be compared with the prediction of conformal field theory. The observed critical exponent η_z in table II is a fit $M_{zz}(\pi/2, \omega) = a + \omega^{\eta_z - 2}$ from the data of the lowest and the second lowest excitations $m = 1, 2$. Conformal field theory predicts that it is equal to the scaled energy gap $2\theta_z = \Omega_z/(\pi v)$.¹⁹ Ω_z and the spin-wave velocity v are defined by the scaled lowest excitation energy at $q = \pi/2$ and $q = 2\pi/N$ in the thermodynamic limit:

$$\begin{aligned}\Omega_z &= \lim_{N \rightarrow \infty} N\omega(m=1, q=\pi/2) \\ 2\pi v &= \lim_{N \rightarrow \infty} N\omega(m=1, q=2\pi/N).\end{aligned}\tag{12}$$

They are shown for $0 < \Delta \leq 1$ in table II. We can see that the observed singularity and the prediction from conformal field theory agree quite well.

Next we consider the dynamic spin structure factor $S_{zz}(\pi/2, \omega)$, which is obtained by the product of transition rates $M_{zz}(\pi/2, \omega)$ and density of states $D_{zz}(\pi/2, \omega)$. Density of states of $\Psi\Psi^*$ excitations are shown in figure 3(a). It begins with flat function from the lower boundary, and gradually increases toward the singularity at the upper boundary.

The spectral-weight distribution $S_{zz}(\pi/2, \omega)$ is shown in figure 3(b). In the XXX case $\Delta = 1$, it has double singularities at the lower and upper boundary.¹⁶ Almost the same line shapes are observed for $0.7 \leq \Delta < 1$. When we further decrease the value of Δ , a small peak near the upper boundary emerges for $\Delta \leq 0.5$, and grows as Δ is further decreasing. In the limit $\Delta \rightarrow 0$, this peak eventually becomes the singularity at the upper boundary, where the line shape coincides with the density of states.

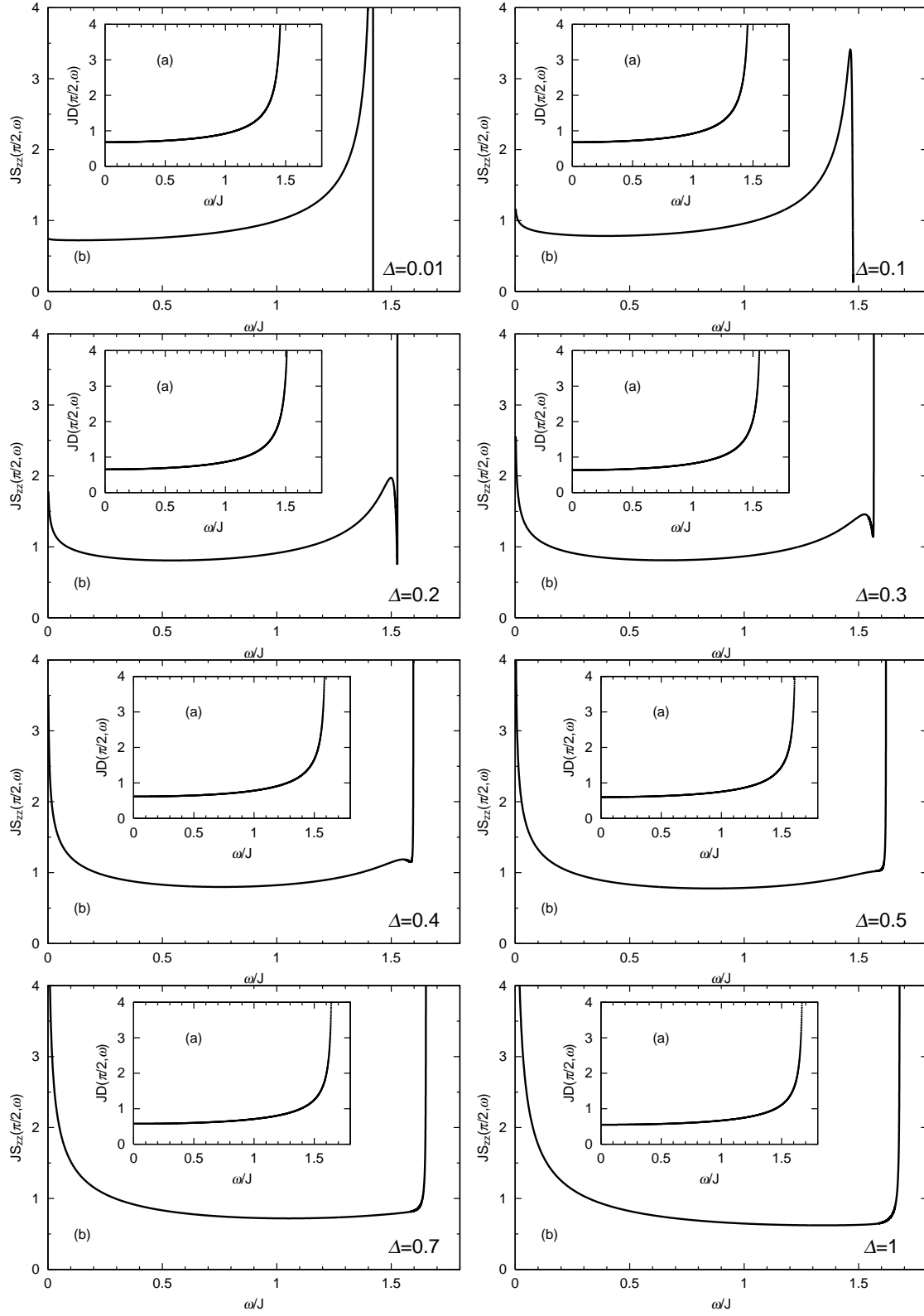


Fig. 3. (a)Density of states for psinon-antipsinon excitations at $q = \pi/2$, $M_z = N/4$ from data for $N=4096$.

(b)Spectral-weight distribution of psinon-antipsinon excitations in $S_{zz}(q, \omega)$ at $q = \pi/2$, $M_z = N/4$ from data for $N=4096$.

5. Conclusion

We have evaluated the longitudinal dynamic spin structure factor $S_{zz}(q, \omega)$ for the massless ($0 < \Delta \leq 1$) spin-1/2 XXZ chain at $q = \pi/2$ with half the saturation magnetization $M_z = N/4$, for the system size $N = 4096$. We have calculated the relative contribution of psinon-antipsinon excitations and confirmed that they are also dominant in the critical regime. We have also seen that the observed critical exponents of the singularity at the lower boundary agree with the prediction of conformal field theory.

We have observed here, for the first time, that the Δ -dependence of transition rates and the spectral weight distribution in the magnetic field. It can be seen that the transition rates coverges toward the constant function with the value 1 in the limit $\Delta \rightarrow 0$. An interesting behavior of line shapes for $S_{zz}(\pi/2, \omega)$ is observed around $0.1 < \Delta < 0.5$, where a small peak emerges near the upper boundary and grows as $\Delta \rightarrow 0$. We hope this peculiar behavior of the peak will be measured in inelastic neutron scattering experiments.

Acknowledgement

We thank K. Sakai for useful discussions. M. S. was supported by Grant-in-Aid for Young Scientists No. 14740228.

References

- 1) H. Bethe, Z. Phys. **71**, 205 (1931).
- 2) M. Takahashi, *Thermodynamics of One-Dimensional Solvable Models*, (Cambridge University Press, Cambridge, 1999).
- 3) P. R. Hammar, M. B. Stone, D. H. Reich, C. Broholm, P. J. Gibson, M. T. nad C. P. Landee, and M. Oshikawa, Phys. Rev. B **59**, 1008 (1999).
- 4) S. E. Nagler, D. A. Tennant, R. A. Cowley, T. G. Perring, and S. K. Satija, Phys. Rev. B **44**, 12361 (1991).
- 5) Th. Niemeijer, Physica **36**, 377 (1967).
- 6) M. B. Stone, D. H. Reich, C. Broholm, K. Lefmann, C. Rischel, C. P. Landee and M. M. Turnbull, Phys. Rev. Lett. **91**, 037205 (2003).
- 7) G. Müller, H. Thomas, H. Beck, and J. C. Bonner , Phys. Rev. B **24**, 1429 (1981).
- 8) A. H. Bougourzi, M. Couture, and M. Kacir, Phys. Rev. B **54**, R12 669 (1996).
- 9) M. Karbach, G. Müller, A. H. Bougourzi, A. Fledderjohann, and K. -H. Mütter, Phys. Rev. B **55**, 12 510 (1997).
- 10) A. H. Bougourzi, M. Karbach, G. Müller, Phys. Rev. B **57**, 11 429 (1998).
- 11) M. Jimbo and T. Miwa, *Algebraic Analysis of Solvable Lattice Models*, (American Mathematical Society, Providence, RI, 1994)
- 12) M. Karbach and G. Müller, Phys. Rev. B **62**, 14 871 (2000).
- 13) M. Karbach, D. Biegel, and G. Müller, Phys. Rev. B **66**, 054405 (2002).
- 14) N. Kitanine, J. M. Maillet, and V. Terras, Nucl. Phys. B **554**, 647 (1999).
- 15) V. E. Korepin, N. M. Bogoliubov and A. G. Izergin, *Quantum Inverse Scattering Method and Correlation Functions*, (Cambridge University Press, Cambridge, 1993).
- 16) D. Biegel, M. Karbach, and G. Müller , Europhys. Lett **59**, 882 (2002).
- 17) D. Biegel, M. Karbach, and G. Müller , J. Phys. A : Math. Gen. **36**, 5361 (2003).
- 18) D. Biegel, M. Karbach, G. Müller and K. Wiele, , Phys. Rev. B **69**, 174404 (2004).
- 19) A. Fledderjohann, C. Gerhardt, K. H. Mütter and A. Schmitt , Phys. Rev. B **54**, 7168 (1996).